# Transglutaminase 2 is upregulated in primary hepatocellular carcinoma with early recurrence as determined by proteomic profiles

HIROMI YAMAGUCHI[1], KAZUMICHI KURODA[2], MASAHIKO SUGITANI[1], TADATOSHI TAKAYAMA[3], KIYOSHI HASEGAWA[4] and MARIKO ESUMI[1]

Divisions of [1]Morphological and Functional Pathology, and [2]Microbiology, Department of Pathology and Microbiology; [3]Department of Digestive Surgery, Nihon University School of Medicine, Itabashi-ku, Tokyo 173-8610; [4]Hepato-Biliary-Pancreatic Surgery Division, Department of Surgery, Graduate School of Medicine, University of Tokyo, Bunkyo-ku, Tokyo 113-8655, Japan

Received August 29, 2016; Accepted February 14, 2017

DOI: 10.3892/ijo.2017.3917

**Abstract.** The mechanism of early recurrence of hepatocellular carcinoma (HCC) is not well understood. To examine whether early intrahepatic metastasis of HCC can be determined by the reliable molecular characteristics of the primary HCC, we focused on early-stage tumors of primary and solitary HCC cases. Proteomic differences were investigated between two groups, 11 early (recurrence within 12 months) and 10 late (no recurrence within 48 months) HCC cases, using two-dimensional fluorescence difference gel electrophoresis. Overall, 10 upregulated and 9 downregulated proteins were identified from a total of 1623 protein spots detected in early recurrent HCC. Cluster analysis using the 19 proteins successfully divided the 21 HCC samples exactly into the two above groups. A multifunctional protein, transglutaminase 2 (TGM2), was upregulated in the early recurrence group. Immunohistochemistry revealed the frequent observation of TGM2-positive HCC cells in the early group, with a tendency of TGM2-positive staining in HCC cells adjacent to fibrous stroma. To examine whether two major TGM2-associated pathways, epithelial-mesenchymal transition (EMT) and integrin signaling, were activated in the early recurrence group of HCC, downstream molecules of TGM2 were measured. The mRNA level of EMT-related genes was highly positively correlated with TGM2 mRNA. However, E-cadherin (CDH1) mRNA and protein were not downregulated in correlation with TGM2 expression. The phosphorylation of FAK and Akt and the downregulation of PTEN were not associated with the quantity of TGM2. Therefore, TGM2 might contribute to early HCC recurrence through signaling pathways not related to EMT and integrin signaling. The proteomics of strictly classified HCCs would be useful for characterizing pro-metastatic HCC and for developing a new therapeutic target for treatment of metastasis.

*Correspondence to:* Dr Mariko Esumi, Division of Morphological and Functional Pathology, Department of Pathology and Microbiology, Nihon University School of Medicine, 30-1 Ohyaguchikami-cho, Itabashi-ku, Tokyo 173-8610, Japan
E-mail: esumi.mariko@nihon-u.ac.jp

*Key words:* epithelial-mesenchymal transition, integrin signaling, hepatocellular carcinoma, proteomics, recurrence, transglutaminase 2

## Introduction

Hepatocellular carcinoma (HCC) is the seventh most common cancer in the world and the third leading cause of cancer-related deaths (1). Hepatitis B virus (HBV) and hepatitis C virus (HCV) are the main causes of HCC, with the latter being the major cause of HCC in Western countries and in Japan (1,2). Surgical resection is one of the first treatments for HCC, though the long-term survival rate after hepatic resection is poor due to frequent recurrence (1). HCC recurrence arises from multicentric HCC or intrahepatic metastasis (3-5), but Wang *et al* indicated that compared with intrahepatic metastatic HCC, multicentric recurrent HCC is associated with a better prognosis (5). Although some cases of early-stage HCC do not recur for a long period after therapeutic resection, intrahepatic metastasis can in some cases occur early, within 12 months after resection. Thus, a comparative study of these two types of HCC to identify factors that influence early intrahepatic metastasis would be helpful for predicting HCC recurrence.

Several studies have demonstrated that clinicopathological factors, such as tumor size, stage, grade and viral load, are significantly related to intrahepatic recurrence (6-8). Molecular prediction of intrahepatic recurrence has been investigated by gene expression profiling analysis in human HCC tissues, whereby transcriptomics between cases of early and late recurrence was performed; some of these molecules identified, however, were not validated by protein expression in HCC tissues (9-12). In addition, there have been a few proteomic studies focused on the recurrence-related characteristics of HCC (13-15). However, consensus results were not obtained because the backgrounds of the subjects studied were

complex, with the complexity varying by study. For example, both HBV-positive and HCV-positive HCCs were included, and various stages of HCC were included in comparisons between early and late recurrence. Therefore, multicentric HCC and intrahepatic metastatic HCC, which are generated by distinct mechanisms and should be analyzed separately, were not differentiated in previous studies.

In this study, we focused on cases of early-stage HCV-positive HCC and compared the protein profiles of HCC samples obtained at the first therapeutic resection between two groups: early and late recurrence after the first resection. Early recurrence in our study was considered to be intrahepatic metastasis, for which characterization by HCC protein profiles may have been possible. We then performed two-dimensional (2D) gel electrophoretic proteomic analysis between the two groups of HCC to clarify the molecular characteristics of early metastatic HCC.

## Materials and methods

*Liver samples for proteomics*. Cancerous liver tissues were obtained by surgical resection of 41 cases of hepatocellular carcinoma positive for HCV. All cases had solitary tumors less than 6 cm in diameter and no metastasis to lymph nodes or other organs (some vascular invasion-positive samples were included). According to the period from the first resection to recurrence, 11 cases were designated as early recurrence (within 12 months), and 14 cases were designated as late recurrence (no recurrence within 48 months). We performed two-dimensional differential gel electrophoresis (2D-DIGE) analysis using 11 and 10 cases from the early and late recurrence groups, respectively. Our study protocol was approved by the Ethics Committee of our School, and informed consent was obtained from the patients. The HCC samples were stored at -80˚C until use.

*Protein extraction from HCC samples and 2D-DIGE*. Protein was directly extracted from the cancerous liver tissues by homogenization in urea-buffer (7 M urea, 2 M thiourea, 4% w/v 3-(3-cholamidopropyl) dimethylammonio-1-propanesulfonate, 1 mM phenylmethanesulfonyl fluoride, and 30 mM Tris-HCl, pH 9.0) using a microtube homogenizer, followed by incubation at room temperature for 30 min. After sonication and centrifugation, the pH of the supernatant was adjusted to 8.0-9.0 with urea-buffer, pH 9.5. The protein concentration was determined using the Bradford method (Bio-Rad Laboratories, Inc., Hercules, CA, USA) (16). Bovine serum albumin was used as a standard. The extracted protein samples were stored at -80˚C.

A 50-$\mu$g sample of protein was labeled with 300 pmol Cy5 (Minimal Labelling Dye, GE Healthcare, Little Chalfont, UK) and an internal standard (a pool of an equal amount of all samples) with 300 pmol Cy3 (Minimal Labelling Dye, GE Healthcare) according to the manufacturer's instructions. The labeled samples were stored at -80˚C. 2D gel electrophoresis was carried out as previously described (17). Briefly, a mixture of 50 $\mu$g each of the Cy3-labeled internal standard and Cy5-labeled sample was loaded onto a ReadyStrip IPG (pH 4-7, 18 cm length, Bio-Rad Laboratories, Inc.) for isoelectric focusing with a CoolPhoreStar IPG-IEF Type-P (Anatech, Tokyo, Japan).

For separation in the second dimension, sodium dodecyl sulfate-polyacrylamide gel electrophoresis (SDS-PAGE) was carried out using a 12.5% polyacrylamide gel (190 x 173 x 1 mm) with a CoolPhoreStar SDS-PAGE Dual-200 (Anatech). The FLA-5100 Fluorescent Image Analyzer (Fujifilm, Tokyo, Japan) was used for acquisition of the gel images. Spot patterns and spot abundance were analyzed by Progenesis SameSpots (Nonlinear Dynamics, Newcastle upon Tyne, UK).

To determine the abundance of each spot, the fluorescence intensity was calculated as a percent value per gel. To normalize inter-gel differences, the Cy5 percent value was normalized to Cy3 in each spot, and the normalized value was used for the statistical analysis. Significantly different spots between the early and late recurrence groups were selected using one-way analysis of variance ($P<0.05$). Cluster analysis was performed with GeneSpring ver. 13.0 (Agilent Technologies, Santa Clara, CA, USA) using values normalized to the median of all samples.

*Protein identification*. To obtain gels for protein identification, 300-440 $\mu$g non-labeled mixed protein was loaded onto an IPG strip and stained with Deep Purple Total Protein Stain (GE Healthcare) according to the manufacturer's instructions. Differentially expressed protein spots in sufficient abundance were automatically excised, washed and destained using Xcise (Shimadzu Biotech, Kyoto, Japan). The spots were then digested with trypsin, and the peptides were desalinized using pipette-tip columns loaded with C18 resin (ZipTip m-C18, Merck Millipore, Darmstadt, Germany). The peptides were eluted onto a $\mu$Focus MALDI plate (Hudson Surface Technology, Inc., Old Tappan, NJ, USA) for AXIMA-QIT (Shimadzu Biotech) analysis. α-Cyano-4-hydroxycinnamic acid (CHCA) was used as the MALDI-matrix. MALDI-TOF mass spectrometry was performed in the positive reflectron mode at 20-23 kV voltage. Approximately 1000 laser shots of the MS spectra were summed. To validate the protein identification, selected intense peptides were subjected to MS/MS fragmentation.

LC-MS/MS or LC-MALDI analysis was performed for low-abundance protein spots. For LC-MS/MS analysis, peptide samples desalinized with a ZipTip m-C18 were collected in 1.5-ml tubes and dried. The samples were then solubilized in 2% v/v acetonitrile/0.1% v/v formic acid. The peptide samples were loaded onto a 5-cm, 100-$\mu$m inner diameter reversed-phase C18 column (HiQ sil C18W-3, KYA Technologies Corp., Tokyo, Japan) using the DiNA nanoLC system (KYA Technologies Corp.) and separated on-line with a QSTAR XL mass spectrometer (AB SCIEX Ltd., Framingham, MA, USA) using a 40-min linear gradient from 2% v/v acetonitrile/0.1% v/v formic acid to 41% v/v acetonitrile/0.1% v/v formic acid.

For LC-MALDI analysis, the trypsinized peptide samples were separated using a Prominence nano (Shimadzu Biotech). A 15-cm column with a 100-$\mu$m inner diameter, MonoCap® for Fast-flow column (GL Sciences Inc., Tokyo, Japan), was used for separation with a 30-min gradient from 5% v/v acetonitrile/0.1% v/v trifluoroacetic acid to 43.25% v/v acetonitrile/0.1% v/v trifluoroacetic acid. The separated peptide samples were automatically spotted onto a $\mu$Focus MALDI plate using AccuSpot (Shimadzu Biotech). One microliter of a CHCA matrix solution (0.5 $\mu$g/$\mu$l) was applied and crystallized, and then MALDI-TOF-MS was automatically

Table I. Primer sequences of the 7 genes examined in this study.

| Accession no. | Symbol | Primer sequence/TaqMan assay ID | Product size (bp) |
|---|---|---|---|
| NM_004613.2 | TGM2 | F: TCCCCACTCACCCCCTTTGC<br>R: TTCCTCTCTCACCCCAGCCC | 93 |
| NM_000660.5 | TGFB1 | F: CATGGGGGCTGTATTTAAGG<br>R: GGGCAAAGGAATAGTGCAGA | 190 |
| NM_001530.3 | HIF1A | F: ACCACTACCACTGCCACCAC<br>R: CCTTTTCCTGCTCTGTTTGG | 182 |
| NM_005985.3 | SNAI1 | F: GGCCTAGCGAGTGGTTCTTC<br>R: TAGGGCTGCTGGAAGGTAAA | 169 |
| NM_003068.4 | SNAI2 | F: ATGAGGAATCTGGCTGCTGT<br>R: GGCTTCGGAGTGAAGAAATG | 84 |
| NM_004360.3 | CDH1 | F: TGGCTTCCCTCTTTCATCTC<br>R: TAGTTCCGCTCTGTCTTTGG | 171 |
| NR_003286.2 | 18S | Hs99999901_s1 | |

F, forward; R, reverse.

Table II. Clinicopathological features of the two groups of early and late recurrence used in this study.

| | Proteomics | | | IHC | | | mRNA quantification | | |
|---|---|---|---|---|---|---|---|---|---|
| Features | Early (n=11) | Late (n=10) | P-value | Early (n=13) | Late (n=20) | P-value | Early (n=9) | Late (n=6) | P-value |
| Male/female | 7/4 | 6/4 | 1.000 | 10/3 | 15/5 | 1.000 | 8/1 | 5/1 | 1.000 |
| Age (range) | 68.6 (61-75) | 66.3 (59-72) | 0.242 | 68.1 (54-75) | 63.8 (49-71) | 0.031[a] | 63.8 (54-78) | 63.8 (51-68) | 0.800 |
| ICG-R15 (%) (<10) | 21.1±2.5 | 16.2±1.5 | 0.314 | 17.9±2.3 | 14.5±1.1 | 0.518 | 19.9±5.5 | 11.8±2.2 | 0.491 |
| Alb (g/dl) (6.7-8.3) | 3.60±0.12 | 3.69±0.10 | 0.640 | 3.74±0.13 | 3.92±0.12 | 0.356 | 3.89±0.17 | 4.37±0.21 | 0.061 |
| AST (IU/l) (8-38) | 68.0±6.0 | 44.8±4.0 | 0.006[a] | 60.8±5.4 | 48.5±3.6 | 0.092 | 61.9±8.7 | 43.5±4.7 | 0.145 |
| ALT (IU/l) (40-44) | 59.2±6.7 | 49.4±7.2 | 0.258 | 54.6±5.92 | 50.0±4.5 | 0.709 | 72.4±15.7 | 46.2±6.8 | 0.137 |
| T. bil (mg/dl) (0.3-1.2) | 0.73±0.08 | 0.85±0.08 | 0.394 | 0.68±0.06 | 0.77±0.06 | 0.471 | 0.77±0.07 | 0.75±0.10 | 0.798 |
| AFP (ng/ml) (<10) | 302±177 | 1497±1460 | 0.436 | 355±172 | 790±729 | 0.579 | 1495±1025 | 61±32 | 0.088 |
| Cirrhosis (-/+) | 4/7 | 8/2 | 0.080 | 3/10 | 11/9 | 0.087 | 2/7 | 4/2 | 0.136 |
| Tumor size (mm) | 30.8±2.7 | 37.1±4.2 | 0.229 | 33.0±2.8 | 29.1±2.8 | 0.223 | 33.7±3.3 | 22.8±3.9 | 0.028[a] |
| Tumor grade (W/M/P) | 3/7/1 | 2/8/0 | 1.000 | 4/8/1 | 5/14/1 | 0.854 | 3/6/0 | 0/3/3 | 0.061 |

Liver functions are expressed as the mean ± SE, and their normal values are shown in parentheses. ICG-15, indocyanine green retention at 15 min; Alb, serum albumin; AST, serum aspartate aminotransferase; ALT, serum alanine aminotransferase; T. bil, total bilirubin; AFP, α-fetoprotein; W, well-differentiated; M, moderately differentiated; P, poorly differentiated; IHC, immunohistochemistry; [a]P<0.05 by the statistical analysis. The value of ICG-R15 was not available from a case of the early recurrence group in the study of IHC and mRNA quantification.

performed (AXIMA Performance, Shimadzu Biotech). All acquired peptide MS or MS/MS data were analyzed with the database search engine MASCOT (Matrix Science Inc., Boston, MA, USA). Protein and peptide identification was based on the MASCOT definition.

*Immunohistochemistry (IHC).* Thirty-three cases were subjected to IHC: 13 and 20 cases of early and late recurrence, respectively, of which 2D-DIGE analysis was performed for 10 and 6 cases, respectively. IHC was performed using formalin-fixed paraffin-embedded tissues, as previously described (18), with some modifications. For antigen retrieval, the sections were treated with 10 mM citrate buffer (pH 6.0) at 120˚C for 15 min for transglutaminase 2 (TGM2) or with 1X Target Retrieval Solution High pH (pH 9.0) (Dako, Glostrup, Denmark) at 120˚C for 15 min for E-cadherin (CDH1). The first antibody reaction was performed with a 1/100 dilution of anti-human TGM2 (rabbit monoclonal, ab109200, Abcam, Cambridge, UK) or a 1/50 dilution of anti-human CDH1 (mouse monoclonal, M3612, Dako) at 37˚C for 60 min; the

second antibody was reacted using Histofine Simple Stain MAX PO (MULTI; Nichirei, Tokyo, Japan) for 30 min at room temperature. The TGM2-positivity was determined using all fields of view (FOVs, 2.2-mm in diameter per FOV) containing HCC (15-107 FOVs per case) as follows: TGM2-positive HCC cells were observed in at least two different FOVs per HCC. According to the staining intensity, semi-quantitative scores were defined as follows: 0, negative; 1, weakly positive; 2, moderately positive; 3, strongly positive.

*Quantification of mRNA*. In addition to the cases used for 2D-DIGE, another 15 cases were subjected to mRNA quantification: 9 and 6 cases from the early and late recurrence groups, respectively. Total RNA was isolated from frozen liver tissues and subjected to DNase I treatment, followed by cDNA synthesis, as previously described (19). Quantitative real-time polymerase chain reaction (qPCR) was performed as previously described (20) with minor modifications; for an internal standard gene, 18S rRNA was quantified with TaqMan gene expression assays using 1 ng cDNA. The expression levels of the target gene mRNAs were determined by qPCR using THUNDERBIRD® SYBR qPCR Mix (TOYOBO Co., Ltd., Osaka, Japan) following the manufacturer's protocol. SNAI1 and TGFB1 were quantified using 50 ng cDNA, and other target genes were quantified using 10 ng cDNA. The primer sequences and TaqMan assay IDs used in this analysis are shown in Table I. The quantity of mRNA was normalized against the quantity of 18S rRNA by the relative quantitation ($\Delta$Ct) method, as previously described (20).

*Western blot analysis*. Western blotting was carried out as previously described (17). Briefly, 20 $\mu$g of protein extracted in urea-buffer for 2D-DIGE was separated on SDS-10% polyacrylamide gels and transferred to a polyvinylidene difluoride membranes. The membranes were incubated with antibodies and then with horseradish peroxidase-conjugated secondary antibodies. The target protein was detected by ImmunoStar Zeta or LD (Wako Pure Chemical Industries, Ltd., Osaka, Japan). The chemiluminescence was acquired and quantified. The first antibodies were as follows: 1/10,000 dilution of anti-human TGM2 (rabbit monoclonal, ab109200, Abcam), 1/1,000 dilution of anti-human PTEN (rabbit monoclonal, #9188, Cell Signaling Technology, Inc., Danvers, MA, USA), 1/1,000 dilution of anti-human phospho-Akt (Ser473) (rabbit monoclonal, #4060, Cell Signaling Technology), 1/3,000 dilution of anti-human pan-Akt (rabbit monoclonal, #4691, Cell Signaling Technology), 1/1,000 dilution of anti-human phospho-FAK (Tyr397) (rabbit monoclonal, #8556, Cell Signaling Technology), 1/2,000 dilution of anti-human FAK (rabbit monoclonal, ab40794, Abcam) and 1/10,000 dilution of anti-human GAPDH (rabbit polyclonal, ab37168, Abcam). The chemiluminescence of TGM2 and PTEN was normalized against that of loading control GAPDH. The phosphorylation rate of FAK and Akt was calculated as a fraction of total FAK and total Akt, respectively.

*Statistical analyses*. Sex, cirrhosis and tumor grade were analyzed by the $\chi^2$-test or Fisher's exact test, and other clinicopathological features were analyzed by the Mann-Whitney U-test. Comparisons of the mRNA and protein levels were analyzed by Student's t-test, and the correlation of the mRNA and protein levels between TGM2 and other genes was analyzed by Spearman's rank correlation coefficient. The immunohistochemical scores for TGM2 were assessed by the Mann-Whitney U test and $\chi^2$-test. A difference was considered significant if the P-value was $<0.05$. All statistical analyses were performed using SPSS Statistics 19 (IBM, Armonk, NY, USA).

## Results

*Comparison of clinicopathological features of HCC cases between early and late recurrence groups*. To characterize HCC prone to intrahepatic metastasis, we isolated 41 rare cases at an early stage of primary and solitary HCC; the average diameter was 32 mm. All cases were positive for HCV because the HCC proteomics clearly differentiated between HBV-positive and HCV-positive tumors (21). Among the 41 cases, 11 recurred early, within 12 months, despite therapeutic resection; these cases are considered to potentially have characteristics that predispose to intrahepatic metastasis compared with the 10 cases that showed no recurrence within 48 months after therapeutic resection (Fig. 1). Comparison of the clinicopathological features between the two groups (Table II) showed no significant difference, except for AST (P=0.006).

*Differential proteins of HCC between early and late recurrence groups*. Twenty-one 2D-DIGE gel images were compared between the early and late recurrence groups, and 1623 spots were detected by Progenesis SameSpots (Fig. 2). Among these 1623 spots, the normalized volumes of 51 were significantly different between the 2 groups; 18 spots were upregulated and 33 spots downregulated in the early group. Of these, we identified 10 upregulated and 9 downregulated proteins that were expressed in a sufficient quantity for identification (Table III). Although the fold change in differential expression for these proteins was not very high, at less than 3-fold, the expression profiles of the 51 differential protein spots and of the 18 identified spots classified the 21 HCC samples exactly into the two groups of recurrence (Fig. 3). Therefore, these proteins might be associated with intrahepatic recurrence of HCV-positive HCC.

*Immunohistochemistry of TGM2*. TGM2 was found to be a significantly upregulated protein in the early group. To determine the localization of TGM2 and to validate this differential expression, we examined TGM2 IHC 33 HCC tissues; the clinicopathological features between 13 early and 20 late recurrence cases are compared in Table II. In most HCC cases, intra-tumor vascular endothelial cells were positive for TGM2 (data not shown). HCC cells were also positive for TGM2, though the frequency of positivity differed by case (Fig. 4). In addition, the TGM2-positive HCC cells tended to be adjacent to fibrous stroma (Fig. 4A). When the TGM2 positivity was semi-quantitatively scored (Fig. 4A), TGM2-positive HCC cells were significantly increased in the early recurrence group compared with those of the late recurrence group (Fig. 4B) (Table IV).

*TGM2-associated pathways in HCC*. TGM2 is a multifunctional protein involved in many biological processes, such

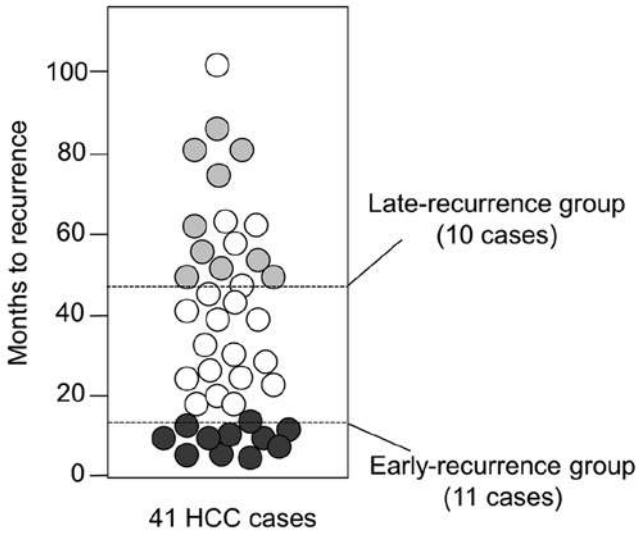


Figure 1. Scatter plot of recurrence periods in 41 HCC cases. Eleven cases of early recurrence within 12 months (dark gray circle) and 10 cases of no recurrence within 48 months (light gray circle) were examined in this study.

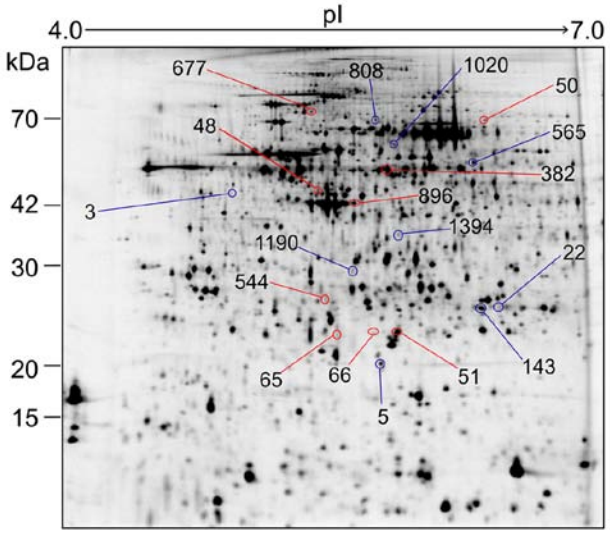


Figure 2. Representative 2D-DIGE gel image of protein extracts from HCCs. The number of spots was automatically provided by the software Progenesis SameSpots. Eighteen protein spots differentially expressed between early and late recurrence groups are indicated on the gel image. Red and blue circles indicate upregulated and downregulated spots in the early recurrence group, respectively.

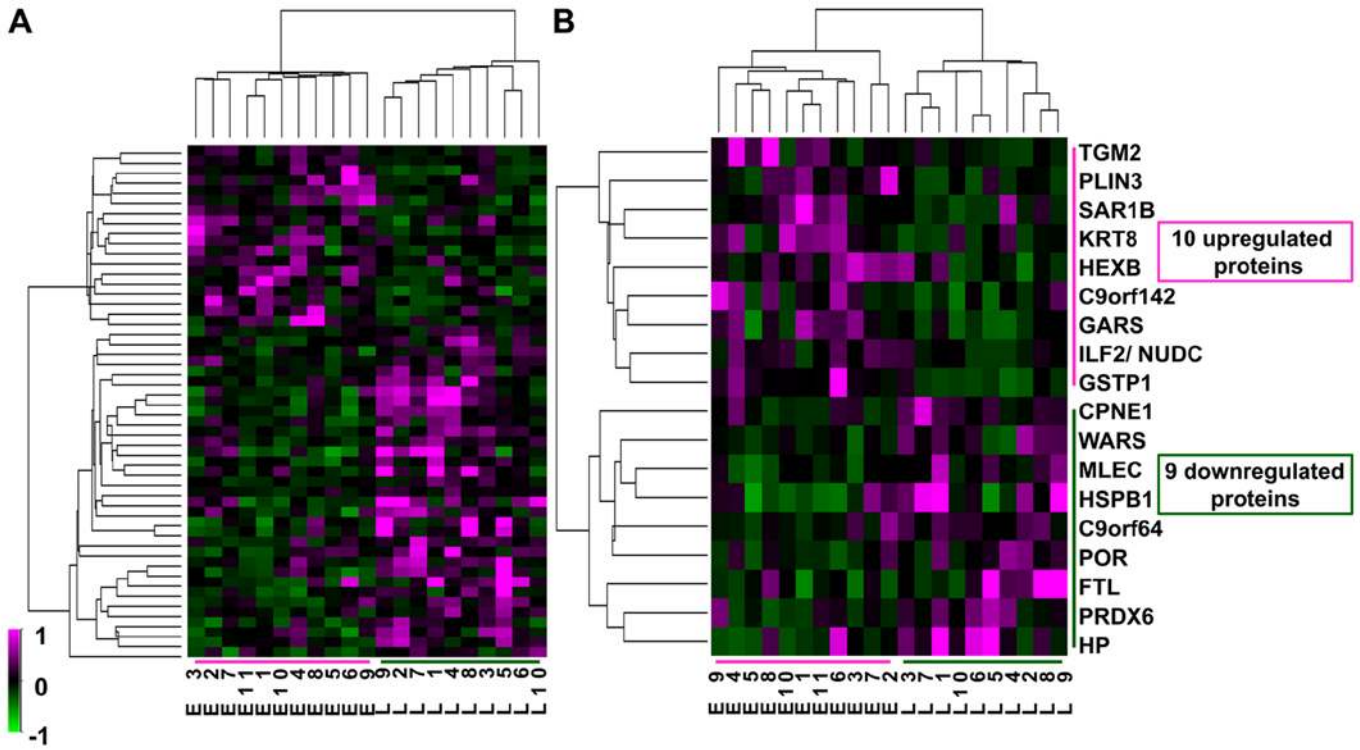


Figure 3. Cluster analyses of 21 HCC samples based on the expression profiles of 51 protein spots (A) and 18 identified spots (B). Each spot volume was normalized by the median value of all samples, and the normalized value is expressed as an exponential notation. E1-11, HCC samples of the early recurrence group; L1-10, HCC samples of the late recurrence group.

as angiogenesis, cell adhesion, migration, survival and the epithelial-mesenchymal transition (EMT) (22). Thus, we investigated two major TGM2-mediated pathways that might influence tumor recurrence (Fig. 5A). EMT plays an important role in tumor metastasis (23). To examine whether upregulation of TGM2 is associated with EMT, we measured mRNA expression of five genes, *TGFB1, HIF1A, SNAI1, SNAI2* and *CDH1*, related to EMT, and the mRNA levels were compared between the two groups; Table II shows the clinicopathological comparison of 9 early and 6 late recurrence cases. TGFB1 signaling and hypoxia induce EMT-inducer genes, such as *SNAI1* and *SNAI2*, and then these transcription factors downregulate E-cadherin (24,25). *TGM2* mRNA is also upregulated by TGFB and HIF1 (26), and the TGM2 protein

Table III. Upregulated and downregulated proteins in the early recurrence group.

A, Upregulated proteins

| Spot no. | P-value | Fold change | Protein ID | Protein | Gene | Function | Score | | | | |
|---|---|---|---|---|---|---|---|---|---|---|---|
| | | | | | | | MALDI-MS | MALDI-MS/MS | | LC-MS/MS | LC-MALDI |
| | | | | | | | | Peak (m/z) | Score | | |
| 677 | 0.047 | 1.6 | P21980 | Protein-glutamine γ-glutamyltransferase 2 | TGM2 | Protein cross-linking | 105 | | | | |
| 51 | 0.001 | 1.4 | P09211 | Glutathione S-transferase P | GSTP1 | The electrophiles detoxification | 74 | 1337.7<br>1550.9<br>1883.9 | 41<br>38<br>61 | | |
| 382 | 0.022 | 1.4 | P05787 | Keratin, type II cytoskeletal 8 | KRT8 | Intermediate filament | 198 | | | | |
| 544 | 0.026 | 1.4 | P07686 | β-hexosaminidase subunit β | HEXB | Ganglioside GM2 degradation | | | | 165 | |
| 48 | 0.028 | 1.4 | O60664 | Perilipin-3 | PLIN3 | Protein transport | | | | 285 | |
| 66 | 0.030 | 1.4 | Q9Y6B6 | GTP-binding protein SAR1b | SAR1B | Protein transport | | | | 90 | |
| 50 | 0.031 | 1.4 | P41250 | Glycine-tRNA ligase | GARS | tRNA aminoacylation | | | | | 311 |
| 65 | 0.039 | 1.4 | Q9BUH6 | Protein PAXX | C9orf142 | DNA double-strand break repair | | | | 124 | |
| 896 (mixed) | 0.044 | 1.2 | Q12905 | Interleukin enhancer -binding factor 2 | ILF2 | Interleukin 2 gene transcription regulator | | | | 95 | |
| | | | Q9Y266 | Nuclear migration protein nudC | NUDC | Mitotic spindles formation | | | | 224 | |

B, Downregulated proteins

| Spot no. | P-value | Fold change | Protein ID | Protein | Gene | Function | Score | | | | |
|---|---|---|---|---|---|---|---|---|---|---|---|
| | | | | | | | MALDI-MS | MALDI-MS/MS | | LC-MS/MS | LC-MALDI |
| | | | | | | | | Peak (m/z) | Score | | |
| 3 | 0.027 | 2.7 | P00738 | Haptoglobin | HP | Iron homeostasis | | | | 134 | |
| 5 | 0.028 | 1.9 | P02792 | Ferritin light chain | FTL | Iron homeostasis | 140 | 1607.8 | 81 | | |
| 143 | 0.040 | 1.6 | P04792 | Heat shock protein β-1 | HSPB1 | Anti-oxidative stress | | 1906.0 | 36 | | 218 |
| 1190 | 0.012 | 1.4 | Q14165 | Malectin | MLEC | Protein glycosylation | 68 | 1592.8 | 58 | | |
| 22 | 0.020 | 1.4 | P30041 | Peroxiredoxin-6 | PRDX6 | Anti-oxidative stress<br>Phospholipid turnover regulation | | | | 81 | |
| 565 | 0.048 | 1.3 | P23381 | Tryptophan-tRNA ligase, cytoplasmic | WARS | tRNA aminoacylation<br>Angiogenesis regulation | 83 | | | | |
| 1020 | 0.020 | 1.3 | Q99829 | Copine-1 | CPNE1 | Membrane trafficking<br>NF-κB transcription repressor | | | | 197 | |
| 808 | 0.043 | 1.2 | P16435 | NADPH-cytochrome P450 reductase | POR | Electron transfer to cytochrome P450 | | | | 276 | |
| 1394 | 0.048 | 1.2 | Q5T6V5 | UPF0553 protein C9orf64 | C9orf64 | Unknown | 99 | | | | |

The number of spots was automatically provided by Progenesis SameSpots. Protein ID indicates accession number in the UniProt/Swiss-Prot database. Protein and peptide scores were obtained from the MASCOT database.

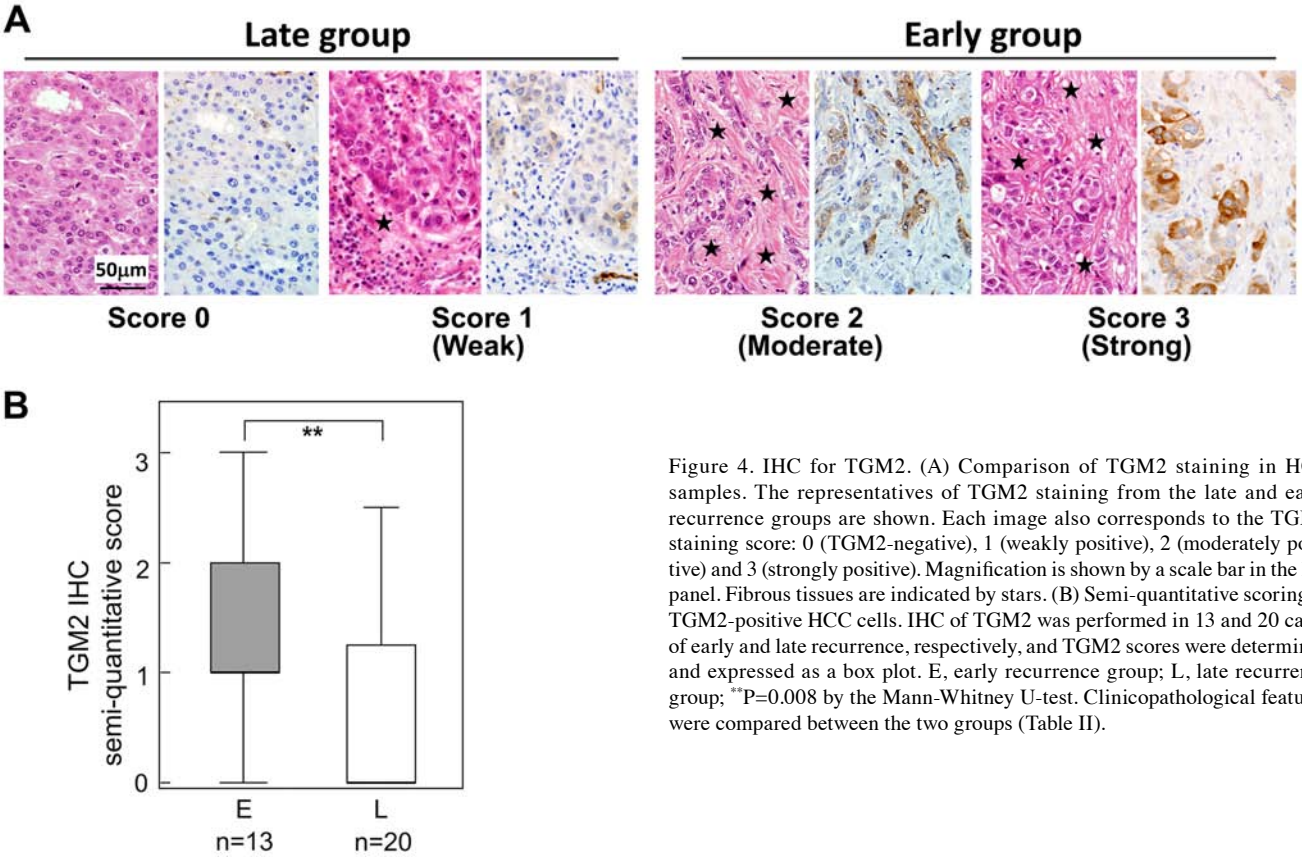


Figure 4. IHC for TGM2. (A) Comparison of TGM2 staining in HCC samples. The representatives of TGM2 staining from the late and early recurrence groups are shown. Each image also corresponds to the TGM2 staining score: 0 (TGM2-negative), 1 (weakly positive), 2 (moderately positive) and 3 (strongly positive). Magnification is shown by a scale bar in the left panel. Fibrous tissues are indicated by stars. (B) Semi-quantitative scoring of TGM2-positive HCC cells. IHC of TGM2 was performed in 13 and 20 cases of early and late recurrence, respectively, and TGM2 scores were determined and expressed as a box plot. E, early recurrence group; L, late recurrence group; $^{**}$P=0.008 by the Mann-Whitney U-test. Clinicopathological features were compared between the two groups (Table II).

Table IV. TGM2 expression in HCC in the early and late recurrence groups.

| | TGM2 expression in HCC | | | |
|---|---|---|---|---|
| | Negative | Positive | Total | P-value |
| Early | 2 | 11 | 13 | 0.004 |
| Late | 14 | 6 | 20 | |
| Total | 16 | 17 | 33 | |

IHC of TGM2 was performed as described in Fig. 4, and positive was defined as TGM-positive HCC cells observed in at least two FOVs. P-value was determined by the $\chi^2$-test.

negatively regulates *CDH1* at the transcriptional level (27). Correlation analyses revealed that the *TGM2* mRNA level was strongly correlated with *TGFB1* and moderately with *HIF1A* and *SNAI1* (Fig. 5B). *CDH1* was also strongly correlated with *TGM2* (Fig. 5B). In addition, the expression levels of these EMT-related genes were not significantly different between the early and late groups (Fig. 5C). IHC showed that the CDH1-staining pattern did not depend on negative staining of TGM2; TGM2-positive and CDH1-negative HCC cells were not consistently observed (Fig. 5D).

On the other hand, TGM2 also activates integrin signaling pathways (Fig. 5A). Such TGM2-mediated integrin signaling enhances not only tumor cell adhesion and migration but also survival and growth (28). Focal adhesion kinase (FAK) and protein kinase B (Akt) are the downstream targets of TGM2-mediated integrin signaling. In addition, TGM2 downregulates the tumor suppressor phosphatase PTEN at a protein level and subsequently leads to the phosphorylation of FAK and Akt (29). Therefore, we examined whether the FAK and Akt proteins were phosphorylated and whether PTEN was downregulated in the HCC tissues of the early recurrence group. Western blot analysis confirmed the upregulation of TGM2 in the early recurrence group of HCC (Fig. 6A and B, P=0.06 by Student's t-test). However, the phosphorylation rates of FAK and Akt were not significantly different between the early and late recurrence groups (Fig. 6B) and were not correlated with the TGM2 abundance (Fig. 6C). The PTEN expression was also similar between the recurrence groups (Fig. 6B) and was not downregulated in correlation with the TGM2 expression (Fig. 6C).

## Discussion

To strictly characterize intrahepatic metastasis of HCC, this study focused on primary, solitary and early-stage HCC cases that were positive for HCV. We then compared the proteomes of two groups of HCC cases: those recurring early and those recurring late. We identified 10 upregulated and 9 downregulated proteins in the early recurrence group (Table III). As the expression profiles of these proteins discriminated the two groups, i.e., early and late recurrence (Fig. 3), it is clear that HCCs recurring early and late have individually characteristic proteins. These proteins are related to a variety of functions, such as iron storage, antioxidant activity, protein transport

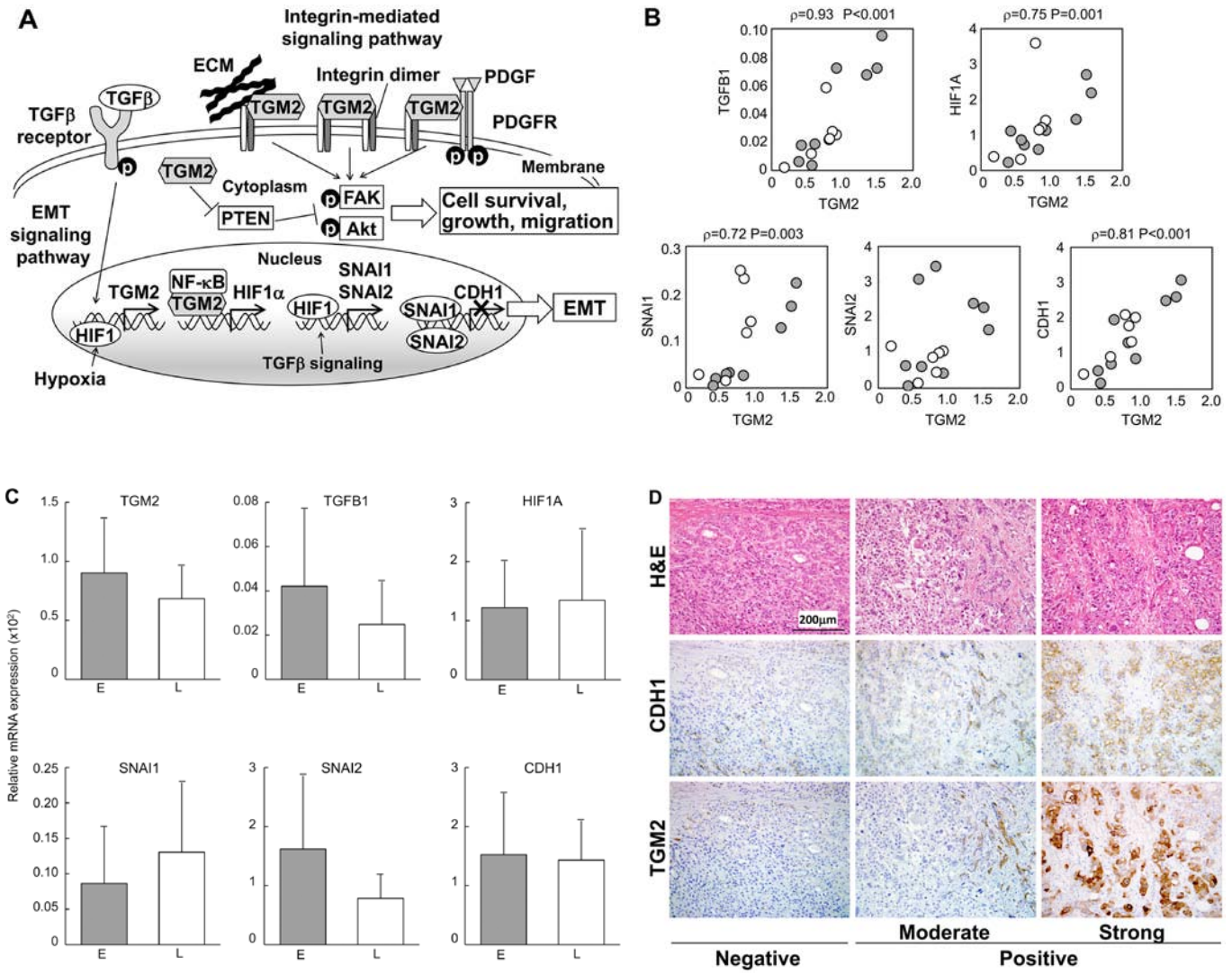


Figure 5. TGM2-associated pathways and downstream gene expression related to EMT. (A) TGM2 mediates the EMT and integrin pathways. TGFβ signaling and HIF1 induce the transcriptional activation of the TGM2. Upregulated TGM2 protein forms a complex with NF-κB and then translocates to the nucleus to promote HIF-1α transcription. Increased HIF1α induces the expression of transcription factors such as SNAI1 and SNAI2, which transcriptionally repress the E-cadherin. On the cell surface, TGM2 interacts with both integrins and extracellular matrix (ECM) proteins such as fibronectin to mediate stable complex formation and induce integrin-integrin clustering. TGM2 also enhances the PDGFR-integrin association. These interactions activate downstream target proteins such as FAK and Akt by phosphorylation. Furthermore, cytosolic TGM2 downregulates the tumor suppressor PTEN at the protein level and consequently activates FAK and Akt. As a result, TGM2 promotes cell survival, growth and migration. Based on Nurminskaya *et al* (22), Verma *et al* (29) and Agnihotri *et al* (30). (B) mRNA expression of TGM2 and EMT-related genes. The quantity of target mRNA was normalized against that of 18S rRNA, and Spearman's rank correlation coefficient were performed between TGM2 and the other genes. Gray circles indicate 9 cases of early recurrence; white circles indicate 6 cases of late recurrence. (C) mRNA expression of TGM2 and EMT-related genes in the early and late recurrence groups. Two-group comparisons were performed using the Student's t-test. The bar graph represents the mean ± SD. E, early recurrence group; L, late recurrence group. Clinicopathological features were compared between the two groups (Table II). (D) Representative images of H&E staining (upper panels) and corresponding CDH1 (middle panels) and TGM2 (lower panels) staining in HCC samples. Three representative cases are shown: TGM2-negative, TGM2 moderately positive and TGM2 strongly positive HCC cells. Magnification for all the panels is shown by a scale bar in the upper left panel.

and lipid metabolism (Table III), and might be candidates for recurrence markers.

In this study, we concentrated on TGM2 upregulation in HCCs prone to recurrence. This multifunctional protein is related to cancer progression, chemoresistance, invasiveness and metastasis and is upregulated in various cancers (26); therefore, we investigated two major TGM2-mediated pathways that might influence tumor recurrence (Fig. 5A). First, in the EMT pathway, TGM2 signaling negatively regulates CDH1 at the transcriptional level (27,30); thus, because CDH1 downregulation is a characteristic of EMT (24), increases in TGM2 may result in EMT and cancer metastasis promotion (23). However, contrary to the expectation, TGM2 mRNA was positively correlated with CDH1 mRNA rather than negatively correlated, yet co-expression of both proteins was not always observed. Recently, Fang *et al* suggested a new metastatic model of HCC independent of EMT (31). Therefore, upregulation of TGM2 might not be associated with EMT but might contribute to early HCC recurrence via a process not related to EMT. Second, in the integrin signaling pathway, FAK and Akt are downstream target proteins activated by phosphorylation through TGM2-integrin signaling, resulting in the activation of tumor cell growth, survival, motility and invasiveness (22). However, the linkage was not observed in the early recurrence group of HCC.

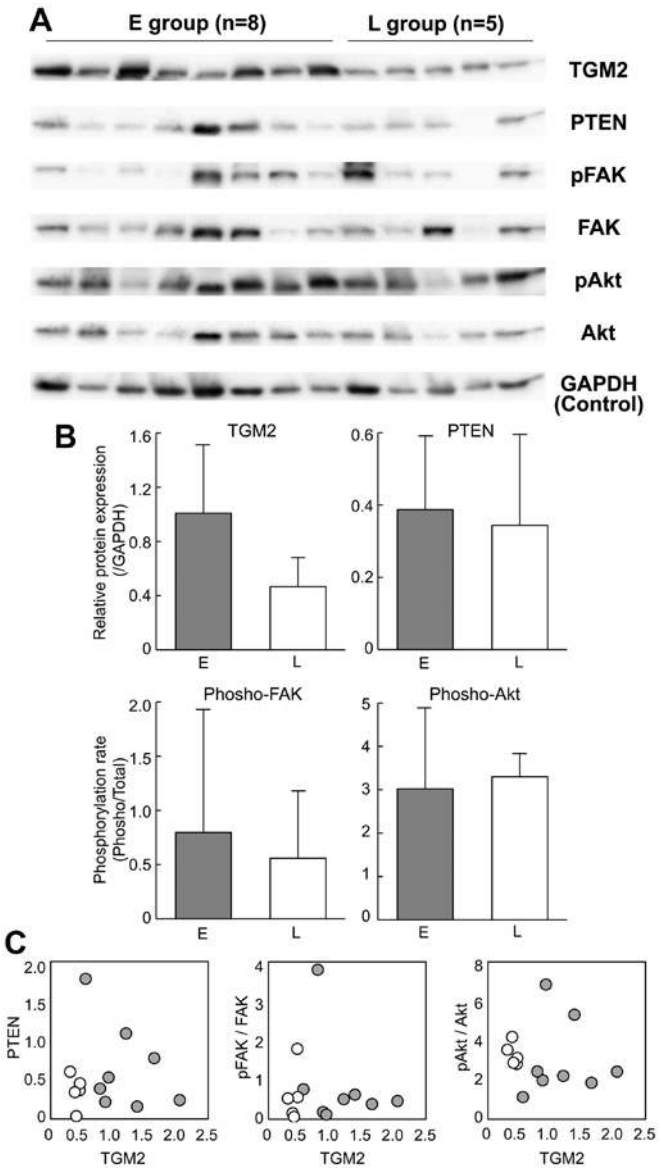


Figure 6. Western blot analysis of the downstream targets of TGM2-mediated integrin signaling. (A) The expression levels of TGM2, PTEN, phospho-FAK (Tyr397), total FAK, phospho-Akt (Ser473) and pan-Akt were analyzed by western blotting. Chemiluminescence was acquired by maximizing the dynamic range. GAPDH was used as a loading control. (B) The relative protein expression of TGM2 and PTEN were normalized against GAPDH using chemiluminescence intensity values and were expressed as an arbitrary unit. The phosphorylation rate of FAK and Akt was also calculated using chemiluminescence intensity values and was expressed as an arbitrary unit. Two-group comparisons were performed using Student's t-test. The bar graph represents the mean ± SD. E, early recurrence group; L, late recurrence group. (C) Spearman's rank correlation analysis was performed between TGM2 and the other proteins. TGM2 and PTEN expression is expressed as the chemiluminescence intensity ($x10^6$), and the phosphorylation rate of FAK and Akt is expressed as the fractions of total FAK and total Akt. Gray circles indicate 8 cases of early recurrence; white circles indicate 5 cases of late recurrence.

Thus, although multiple TGM2-mediated pathways have been clarified in experimental models *in vitro* and *in vivo*, these are not simply observed in human pathological tissues.

Recently, Tatsukawa *et al* demonstrated the complexity of TGM2-mediated signaling (32); multifunctional TGM2 is involved in many cellular processes and has different functions, which vary among organs, cell types and subcellular protein localization (22,32). Even in the liver, TGM2 has opposing roles, such as anti-apoptotic and pro-apoptotic or fibrogenic and anti-fibrogenic roles, depending on the experimental animal model used (32). Thus, it is yet unknown by what molecular mechanism TGM2 is involved in the early recurrence of HCC. Considering our observation of TGM2-positive HCC cells adjacent to fibrous stroma (Fig. 4A), it is possible that TGM2 might be associated with early recurrence via ECM-integrin signaling and 'locally' activates downstream targets such as FAK and Akt. Further analyses are needed to clarify the contribution to early HCC recurrence by TGM2.

Another upregulated protein in the early group, PAXX (the *C9orf142* gene), is involved in repairing DNA double-strand breaks via the non-homologous end joining pathway (33-35). Upregulation of PAXX may indirectly indicate that severe DNA damage is a characteristic of HCC early recurrence.

In contrast, copine-1 (CPNE1), tryptophanyl-tRNA synthetase (WARS) and heat shock protein beta-1 (HSPB1, also known as HSP27) were downregulated in the early group. CPNE1 acts as a transcriptional repressor of NF-κB (36). NF-κB has dual role in HCC, as a tumor promoter and a tumor suppressor (37), but NF-κB overexpression is associated with poor overall survival in most solid tumor cases (38). Thus, downregulation of CPNE1 in early recurrence HCC may result in constitutive NF-κB expression and contribute to a highly malignant phenotype. Ghanipour *et al* reported that low expression of WARS is associated with a metastatic phenotype of colorectal cancer (39). In contrast, WARS was found to be upregulated in malignant ovarian cancer (40) and oral squamous cell carcinoma (41). Thus, Lee *et al* suggested that WARS has paradoxical effect on tumor invasiveness in different tumor types (41).

In the present study, WARS was downregulated in early recurrence HCC; conversely, Taoka *et al* reported WARS upregulation in early recurrent HCC (15). Such an inconsistency was also observed for HSPB1. Upregulation of heat shock proteins such as HSPB1, HSP70 and HSP90 is often observed in many types of cancer, including HCC, due to cancer cell adaptation to stress conditions (42). HSPB1 upregulation has been associated with metastatic or invasive HCC (43), and Taoka *et al* found HSPB1 upregulation in early recurrence HCC (15). However, HSPB1 protein spots in our study indicated downregulation in early recurrence HCC. There are two possibilities for such discrepancies. One possibility is a difference in the clinicopathological factors used for defining early and late recurrence groups, such as tumor size, grade, time to recurrence, and viral infection status. We strictly selected our HCC cases and categorized them into two groups; therefore, such differences in background factors may result in discrepancies. The other possibility is a difference in the proteomic methodology, i.e., protein separation and protein quantification. Taoka *et al* separated protein samples by SDS-PAGE, and all identified peptides corresponding to a single protein, including modified or degraded forms, were used to determine protein abundance (15) by emPAI (44). In contrast, we used the 2D-DIGE method and focused on a single protein spot to i) identify a protein and ii) determine abundance according to the fluorescence intensity. Therefore, it is critical for clinical proteomics to precisely estimate the background clinicopathological features and appropriately incorporate these features into the study.

Overall, this study suggests that TGM2 upregulation is a characteristic of early HCC recurrence and that it might be a helpful marker for the early detection of HCC recurrence.

## Acknowledgements

We are indebted to Dr H. Nakayama (Nihon University School of Medicine) for providing the clinical data of the patients. The human liver samples were provided by Dr T. Mamiya (Nihon University School of Medicine) and Professor N. Kokudo (Graduate School of Medicine, University of Tokyo). We also thank Dr F. Fuchinoue (Nihon University School of Medicine) for helpful suggestions on the pathological data and Ms. Y. Hirotani (Nihon University School of Medicine) for technical assistance. This work was supported by a grant for 'Open Research Center' Project for Private Universities: matching fund subsidy from MEXT (2005), Nihon University Multidisciplinary Research Grants for 2009, and Grant-in-Aid for Scientific Research (C) 25430142 from MEXT (2013). English editorial assistance was provided by American Journal Experts.

## References

1. Yang JD and Roberts LR: Hepatocellular carcinoma: A global view. Nat Rev Gastroenterol Hepatol 7: 448-458, 2010.
2. Ikai I, Arii S, Okazaki M, Okita K, Omata M, Kojiro M, Takayasu K, Nakanuma Y, Makuuchi M, Matsuyama Y, *et al*: Report of the 17th Nationwide Follow-up Survey of Primary Liver Cancer in Japan. Hepatol Res 37: 676-691, 2007.
3. Chen YJ, Yeh SH, Chen JT, Wu CC, Hsu MT, Tsai SF, Chen PJ and Lin CH: Chromosomal changes and clonality relationship between primary and recurrent hepatocellular carcinoma. Gastroenterology 119: 431-440, 2000.
4. Nomoto S, Kinoshita T, Kato K, Otani S, Kasuya H, Takeda S, Kanazumi N, Sugimoto H and Nakao A: Hypermethylation of multiple genes as clonal markers in multicentric hepatocellular carcinoma. Br J Cancer 97: 1260-1265, 2007.
5. Wang B, Xia CY, Lau WY, Lu XY, Dong H, Yu WL, Jin GZ, Cong WM and Wu MC: Determination of clonal origin of recurrent hepatocellular carcinoma for personalized therapy and outcomes evaluation: A new strategy for hepatic surgery. J Am Coll Surg 217: 1054-1062, 2013.
6. Portolani N, Coniglio A, Ghidoni S, Giovanelli M, Benetti A, Tiberio GA and Giulini SM: Early and late recurrence after liver resection for hepatocellular carcinoma: Prognostic and therapeutic implications. Ann Surg 243: 229-235, 2006.
7. Shindoh J, Hasegawa K, Matsuyama Y, Inoue Y, Ishizawa T, Aoki T, Sakamoto Y, Sugawara Y, Makuuchi M and Kokudo N: Low hepatitis C viral load predicts better long-term outcomes in patients undergoing resection of hepatocellular carcinoma irrespective of serologic eradication of hepatitis C virus. J Clin Oncol 31: 766-773, 2013.
8. Cheng Z, Yang P, Qu S, Zhou J, Yang J, Yang X, Xia Y, Li J, Wang K, Yan Z, *et al*: Risk factors and management for early and late intrahepatic recurrence of solitary hepatocellular carcinoma after curative resection. HPB Oxf 17: 422-427, 2015.
9. Iizuka N, Oka M, Yamada-Okabe H, Nishida M, Maeda Y, Mori N, Takao T, Tamesa T, Tangoku A, Tabuchi H, *et al*: Oligonucleotide microarray for prediction of early intrahepatic recurrence of hepatocellular carcinoma after curative resection. Lancet 361: 923-929, 2003.
10. Kurokawa Y, Matoba R, Takemasa I, Nagano H, Dono K, Nakamori S, Umeshita K, Sakon M, Ueno N, Oba S, *et al*: Molecular-based prediction of early recurrence in hepatocellular carcinoma. J Hepatol 41: 284-291, 2004.
11. Wang SM, Ooi LL and Hui KM: Identification and validation of a novel gene signature associated with the recurrence of human hepatocellular carcinoma. Clin Cancer Res 13: 6275-6283, 2007.
12. Yoshioka S, Takemasa I, Nagano H, Kittaka N, Noda T, Wada H, Kobayashi S, Marubashi S, Takeda Y, Umeshita K, *et al*: Molecular prediction of early recurrence after resection of hepatocellular carcinoma. Eur J Cancer 45: 881-889, 2009.
13. Yokoo H, Kondo T, Okano T, Nakanishi K, Sakamoto M, Kosuge T, Todo S and Hirohashi S: Protein expression associated with early intrahepatic recurrence of hepatocellular carcinoma after curative surgery. Cancer Sci 98: 665-673, 2007.
14. Tan GS, Lim KH, Tan HT, Khoo ML, Tan SH, Toh HC and Ching Ming Chung M: Novel proteomic biomarker panel for prediction of aggressive metastatic hepatocellular carcinoma relapse in surgically resectable patients. J Proteome Res 13: 4833-4846, 2014.
15. Taoka M, Morofuji N, Yamauchi Y, Ojima H, Kubota D, Terukina G, Nobe Y, Nakayama H, Takahashi N, Kosuge T, *et al*: Global PROTOMAP profiling to search for biomarkers of early-recurrent hepatocellular carcinoma. J Proteome Res 13: 4847-4858, 2014.
16. Bradford MM: A rapid and sensitive method for the quantitation of microgram quantities of protein utilizing the principle of protein-dye binding. Anal Biochem 72: 248-254, 1976.
17. Yamaguchi H, Hasegawa K and Esumi M: Protein from the fraction remaining after RNA extraction is useful for proteomics but care must be exercised in its application. Exp Mol Pathol 95: 46-50, 2013.
18. Esumi M, Ishibashi M, Yamaguchi H, Nakajima S, Tai Y, Kikuta S, Sugitani M, Takayama T, Tahara M, Takeda M, *et al*: Transmembrane serine protease TMPRSS2 activates hepatitis C virus infection. Hepatology 61: 437-446, 2015.
19. Yamaguchi H, Matsumoto S, Ishibashi M, Hasegawa K, Sugitani M, Takayama T and Esumi M: β-Glucuronidase is a suitable internal control gene for mRNA quantitation in pathophysiological and non-pathological livers. Exp Mol Pathol 95: 131-135, 2013.
20. Numaguchi S, Esumi M, Sakamoto M, Endo M, Ebihara T, Soma H, Yoshida A and Tokuhashi Y: Passive cigarette smoking changes the circadian rhythm of clock genes in rat intervertebral discs. J Orthop Res 34: 39-47, 2016.
21. Kim W, Oe Lim S, Kim JS, Ryu YH, Byeon JY, Kim HJ, Kim YI, Heo JS, Park YM and Jung G: Comparison of proteome between hepatitis B virus- and hepatitis C virus-associated hepatocellular carcinoma. Clin Cancer Res 9: 5493-5500, 2003.
22. Nurminskaya MV and Belkin AM: Cellular functions of tissue transglutaminase. Int Rev Cell Mol Biol 294: 1-97, 2012.
23. Tsai JH and Yang J: Epithelial-mesenchymal plasticity in carcinoma metastasis. Genes Dev 27: 2192-2206, 2013.
24. Naber HP, Drabsch Y, Snaar-Jagalska BE, ten Dijke P and van Laar T: Snail and Slug, key regulators of TGF-β-induced EMT, are sufficient for the induction of single-cell invasion. Biochem Biophys Res Commun 435: 58-63, 2013.
25. Catalano V, Turdo A, Di Franco S, Dieli F, Todaro M and Stassi G: Tumor and its microenvironment: A synergistic interplay. Semin Cancer Biol 23: 522-532, 2013.
26. Huang L, Xu AM and Liu W: Transglutaminase 2 in cancer. Am J Cancer Res 5: 2756-2776, 2015.
27. Shao M, Cao L, Shen C, Satpathy M, Chelladurai B, Bigsby RM, Nakshatri H and Matei D: Epithelial-to-mesenchymal transition and ovarian tumor progression induced by tissue transglutaminase. Cancer Res 69: 9192-9201, 2009.
28. Mangala LS, Fok JY, Zorrilla-Calancha IR, Verma A and Mehta K: Tissue transglutaminase expression promotes cell attachment, invasion and survival in breast cancer cells. Oncogene 26: 2459-2470, 2007.
29. Verma A, Guha S, Wang H, Fok JY, Koul D, Abbruzzese J and Mehta K: Tissue transglutaminase regulates focal adhesion kinase/AKT activation by modulating PTEN expression in pancreatic cancer cells. Clin Cancer Res 14: 1997-2005, 2008.
30. Agnihotri N, Kumar S and Mehta K: Tissue transglutaminase as a central mediator in inflammation-induced progression of breast cancer. Breast Cancer Res 15: 202, 2013.
31. Fang JH, Zhou HC, Zhang C, Shang LR, Zhang L, Xu J, Zheng L, Yuan Y, Guo RP, Jia WH, *et al*: A novel vascular pattern promotes metastasis of hepatocellular carcinoma in an epithelial-mesenchymal transition-independent manner. Hepatology 62: 452-465, 2015.
32. Tatsukawa H, Furutani Y, Hitomi K and Kojima S: Transglutaminase 2 has opposing roles in the regulation of cellular functions as well as cell growth and death. Cell Death Dis 7: e2244, 2016.
33. Xing M, Yang M, Huo W, Feng F, Wei L, Jiang W, Ning S, Yan Z, Li W, Wang Q, *et al*: Interactome analysis identifies a new paralogue of XRCC4 in non-homologous end joining DNA repair pathway. Nat Commun 6: 6233, 2015.
34. Craxton A, Somers J, Munnur D, Jukes-Jones R, Cain K and Malewicz M: XLS (c9orf142) is a new component of mammalian DNA double-stranded break repair. Cell Death Differ 22: 890-897, 2015.

35. Ochi T, Blackford AN, Coates J, Jhujh S, Mehmood S, Tamura N, Travers J, Wu Q, Draviam VM, Robinson CV, *et al*: DNA repair. PAXX, a paralog of XRCC4 and XLF, interacts with Ku to promote DNA double-strand break repair. Science 347: 185-188, 2015.
36. Ramsey CS, Yeung F, Stoddard PB, Li D, Creutz CE and Mayo MW: Copine-I represses NF-kappaB transcription by endoproteolysis of p65. Oncogene 27: 3516-3526, 2008.
37. Xia Y, Shen S and Verma IM: NF-κB, an active player in human cancers. Cancer Immunol Res 2: 823-830, 2014.
38. Wu D, Wu P, Zhao L, Huang L, Zhang Z, Zhao S and Huang J: NF-κB expression and outcomes in solid tumors: A systematic review and meta-analysis. Medicine (Baltimore) 94: e1687, 2015.
39. Ghanipour A, Jirström K, Pontén F, Glimelius B, Påhlman L and Birgisson H: The prognostic significance of tryptophanyl-tRNA synthetase in colorectal cancer. Cancer Epidemiol Biomarkers Prev 18: 2949-2956, 2009.
40. Morita A, Miyagi E, Yasumitsu H, Kawasaki H, Hirano H and Hirahara F: Proteomic search for potential diagnostic markers and therapeutic targets for ovarian clear cell adenocarcinoma. Proteomics 6: 5880-5890, 2006.
41. Lee CW, Chang KP, Chen YY, Liang Y, Hsueh C, Yu JS, Chang YS and Yu CJ: Overexpressed tryptophanyl-tRNA synthetase, an angiostatic protein, enhances oral cancer cell invasiveness. Oncotarget 6: 21979-21992, 2015.
42. Wang C, Zhang Y, Guo K, Wang N, Jin H, Liu Y and Qin W: Heat shock proteins in hepatocellular carcinoma: Molecular mechanism and therapeutic potential. Int J Cancer 138: 1824-1834, 2016.
43. Wang RC, Huang CY, Pan TL, Chen WY, Ho CT, Liu TZ and Chang YJ: Proteomic characterization of Annexin l (ANX1) and heat shock protein 27 (HSP27) as biomarkers for invasive hepatocellular carcinoma cells. PLoS One 10: e0139232, 2015.
44. Ishihama Y, Oda Y, Tabata T, Sato T, Nagasu T, Rappsilber J and Mann M: Exponentially modified protein abundance index (emPAI) for estimation of absolute protein amount in proteomics by the number of sequenced peptides per protein. Mol Cell Proteomics 4: 1265-1272, 2005.